IOP Conference Series: Materials Science and Engineering

PAPER • OPEN ACCESS

Conduction mechanism of Co-doped ZnO transparent memristive devices

To cite this article: Firman Mangasa Simanjuntak *et al* 2021 *IOP Conf. Ser.: Mater. Sci. Eng.* **1034** 012139

View the article online for updates and enhancements.

240th ECS Meeting ORLANDO, FL

Orange County Convention Center Oct 10-14, 2021

Abstract submission due: April 9

SUBMIT NOW

This content was downloaded from IP address 152.78.1.71 on 19/03/2021 at 12:20

Conduction mechanism of Co-doped ZnO transparent memristive devices

Firman Mangasa Simanjuntak[1], Sridhar Chandrasekaran[2], Om Kumar Prasad[3], Femiana Gapsari[4], Themis Prodromakis[1]*, Tseung-YuenTseng[5]**

1 Centre for Electronics Frontiers, University of Southampton, SO171BJ, UK
*Email: t.prodromakis@soton.ac.uk

2 Department of Electrical Engineering and Computer Science, National Chiao Tung University, Hsinchu 30010, Taiwan

3 International College of Semiconductor, National Chiao Tung University, Hsinchu, 30010, Taiwan

4 Mechanical Engineering Department, Brawijaya University, Malang 65145, Indonesia

5 Institute of Electronics, National Chiao Tung University, Hsinchu, 30010, Taiwan
**Email: tseng@cc.nctu.edu.tw

Abstract. The Co dopant substitutes the Zn atomic position in the hexagonal crystal lattice and generates acceptor defects. These defects play significant role in modulating the conduction mechanism of the memristive device. The devices without Co dopant have high concentration of donor defects so that the electron can flow easily through hopping these donor defects; henceforth, only weak filaments can be formed during the set process. Meanwhile, the increase of the acceptor defects in the films enhances the film resistivity. This acceptor defects also contribute to an increase of barrier height at the electrode/dielectric interface where the electrons require higher energy to overcome this barrier and, eventually, induce the formation of strong filaments during the set process.

Keywords: memristive, data storage, ZnO-based devices, transparent electronics.

1. Introduction

Memristive device is one of the emerging non-volatile memory technologies that could be the future data storage; moreover, it could revolutionize computing architecture due to its potential application in artificial intelligence hardware systems as the processing element [1–5]. Various designs of memristive devices having various oxides (HfO_2, ZrO_2, TaOx, etc) and electrodes (metallic and conducting oxides) have been reported [6–16]. Nevertheless, ZnO-based memristive device is recently gain considerable interest not only due to its good switching performance but also its excellent feasibility for fabricating transparent electronics [17–20]. The switching mechanisms of the ZnO-based memristive device is based on filamentary mechanism

Content from this work may be used under the terms of the Creative Commons Attribution 3.0 licence. Any further distribution of this work must maintain attribution to the author(s) and the title of the work, journal citation and DOI.
Published under licence by IOP Publishing Ltd

[21,22]; the filament is formed due to the arrangement of the oxygen vacancies under an electric field as the conduction path for the electrons to flow through the dielectric [23]. Note that beside donor defects, the acceptor defects also play crucial role in this process. Recently, we investigated the impact of acceptor dopants on the switching characteristics of the memristive devices and we found that a moderate concentration of Co dopants can significantly enhance the switching performance [24]. The addition of Co into the ZnO system induce the formation of various acceptor defects such as zinc vacancies and oxygen interstitials; the dopants also reduce the concentration of oxygen vacancies and zinc interstitials [24]. Despite the relationship between point defects and the switching characteristics have been well investigated, the detail conduction mechanism on how the electrons flow in the devices during switching is still not discussed. This letter reports the role of the doping technique in modulating the electron conductions in the ITO/Co:ZnO/ITO system.

2. Methods

All film deposition was conducted using radio frequency sputtering technique; this technique was chosen due to its lower cost, non-toxic, and good reproducibility process as compared to other techniques [19]. The fabrication flow is depicted in **Figure 1**. Cobalt-doped Zinc oxide powder target were prepared in various weight molar percentage of CoO (0, 2, and 5 mol%) and ZnO (99.9, 0.98 and 0.95 mol%). In brief, the ratio of each Co:ZnO mixed in ethanol 99.99% purity by using a ball-milling on homogeneous stirring for 24 hours. Later, the following ratio was dried in a conventional oven at 85 ^{0}C in the air. The dried Co:ZnO powder gently multure using an agate mortar and pestle. The powders are then annealed at 1200 ^{0}C along 2 hours in air ambient; heating rate is 5 °C min^{-1}. Again, the calcined powder is cultured using an agate mortar. Thereafter, Co:ZnO powder compressed under 3-inches diameter magnetron holder plate by uniaxial pressed with a load of 1000 kgf for one hour. Finally, the RF-magnetron sputter was used to form 37 nm Co:ZnO switching layer on ITO-coated commercial glass, (ITO act as bottom electrode). The deposition parameters for switching layer are: 60 Watt RF power, 10 mTorr working pressure, ambient condition Ar:O_2 (2:1) with a total flow rate of 30 sccm and 50 min deposition time at the room temperature. The 115 nm ITO top electrodes were deposited by RF sputtering (100 Watt, 20 sccm Ar ambient, 10 mTorr) pattern with 150 um diameter metal shadow masks. XRD analysis were conducted to examine crystal structure of the synthesized targets. All the electrical characterization was measured using Agilent B1500A semiconductor parameters analyzer.

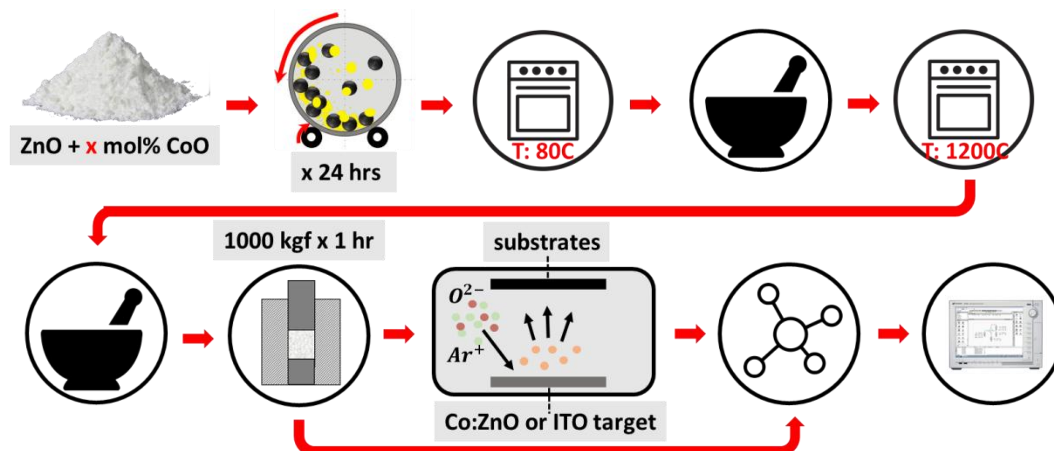

Figure 1. Fabrication and characterization flow of Co-doped ZnO transparent memristive devices

3. Result and discussion

The XRD patterns of the Co:ZnO sputtering targets and the films were carefully investigated and the patterns are matched with hexagonal wurtzite ZnO crystal structure (JCPDS#36-1451), as depicted in **Figure 2 a)** and **Figure 2 b)**, respectively; no formation of Zn_xCo_yO compounds (JCPDS#23-1390) which indicates that the Co dopant successfully substituted Zn potitions in the lattices without transforming the crystal structures in the targets and films. Nevertheless, the increase of Co dopant significantly reduce the (002) orientation in the films (**Figure 2b**) and, thus, the films lose their perpendicular orientation and have more random oriented grains. Figure 2(c) depicts the transparency of the fabricated devices having various concentration of Co dopant. All devices are found to be highly transparent in visible light regions; the average transmittance of 0Co:ZnO, 2Co:ZnO, and 5Co:ZnO are 85.6, 85.08, 84.31, respectively. A slight decrease in transmittance is due to the formation of a more random orientation of the grains in the films having higher Co concentration [24].

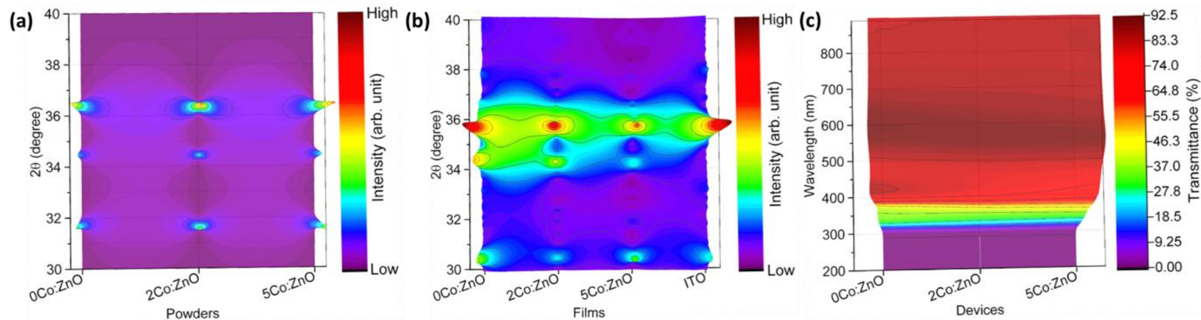

Figure 2. 3-D maps (top view) of X-ray diffraction patterns of Co-doped ZnO in the form of: a) powders and b) films, c) 3-D maps (top view) of UV-visible transmittance spectra of the Co-doped ZnO memristive devices fabricated with various concentration of Co dopant.

The electrical characteristics of the devices were measured by voltage-biasing the top electrodes while the bottom electrodes are grounded (**Figure 3a**). The devices require forming process to activate the switching properties where they switch from pristine resistance state (PRS) to low resistance state (LRS), the devices having higher Co dopant need higher forming voltage (**Figure 3b**) due to the generation of acceptor defects that result in an increase of film resistivity [24]. The devices exhibit counter-clockwise bipolar switching properties and the devices can be switched to the high resistance state (HRS) and LRS by sweeping negative and positive voltage biases, respectively (**Figure 3c**). The detail of the switching performance of these devices and their relationship to the films microstructures and defects can be found in our previous report [24]. In order to investigate on how the electrons flow in the devices, we carefully fitted the LRS and HRS curves with all possible conduction mechanisms that may responsible in the switching process. Generally, electron tunneling follows Schottky emission (SE), Frenkel-Pool emission (FPE), Fowler-Nordhiem tunneling (Field emission, FE), ionic conduction (IC), space charge limited conduction (SCLC), Ohmic conduction (OC) and direct tunneling (DT) [25,26]; their relationships are explained in equation 1 to 7.

$$J_{SE} = A^{*}T^{2}exp\left[\frac{-q\left(\emptyset_B-\sqrt{qE/4\pi\varepsilon_0\varepsilon_r}\right)}{kT}\right] \sim T^{2}exp\left(\frac{+a\sqrt{V}}{T}-\frac{q\emptyset_B}{kT}\right) \quad (1)$$

$$J_{FPE} = E\ exp\left[\frac{-q\left(\emptyset_B-\sqrt{qE/\pi\varepsilon_0\varepsilon_r}\right)}{kT}\right] \sim V\ exp\left(\frac{+2a\sqrt{V}}{T}-\frac{q\emptyset_B}{kT}\right) \quad (2)$$

$$J_{FE} = E^2\ exp\left[\frac{-4\sqrt{2m^*}(q\emptyset_B)^{3/2}}{3q\eta E}\right] \sim V^2 exp\left(-\frac{b}{V}\right) \quad (3)$$

$$J_{IC} = \frac{E}{T}\ exp\left[\frac{-\Delta E_0}{kT}\right] \sim \frac{V}{T}\ exp\left(-\frac{c}{T}\right) \quad (4)$$

$$J_{SCLC} = \zeta\ \frac{\varepsilon}{4\pi}\frac{\mu V^2}{L^3} \sim V^2 \quad (5)$$

$$J_{OC} = E\ exp\left[\frac{-\Delta E_0}{kT}\right] \sim V\ exp\left(-\frac{c'}{T}\right) \quad (6)$$

$$J_{DT} = \frac{BE_{ox}^2}{\left[1-(\emptyset_B-qV_{ox}/\emptyset_B)^{1/2}\right]^2} \exp\left[-\frac{C}{E_{ox}}\frac{\emptyset_B^{3/2}-(\emptyset_B-qV_{ox})^{3/2}}{\emptyset_B^{3/2}}\right] \quad (7)$$

Where the current density, effective Richardson constant, temperature, Boltzmann’s constant, permittivity of the free space, relative dielectric constant, charge of an electron, potential barrier height, free activation enthalpy, oxide electric field, oxide voltage, and thickness are represented as J, A^*, T, k, ε_0, ε_r, q, $\emptyset_B$, ΔE_0, E_{ox}, V_{ox}, and L, respectively.

Figures 3 d-g show the conduction mechanism of 0Co:ZnO device. The electron conduction in HRS curve follows FPE and SCLC mechanism in low and high voltage regions while the LRS curve follows FPE mechanism. Note that the 0Co:ZnO films have high concentration of donor defects [24] and, thus, the electrons may easily flow from cathode to anode by hopping trough the donor defects during set process; moreover, the FPE in LRS curve may suggest that no strong formation of conduction filament after the set process is done. Meanwhile, in the devices having Co dopants (2Co:ZnO and 5Co:ZnO) the HRS curves follow SE and FPE mechanisms and the OC dominates the LRS curves (**Figures 3h-n**). As the Co dopants were introduced into the ZnO crystal lattices, these dopants generate the acceptor defects and increases the barrier height at the ITO/Co:ZnO junction and, consequently, the electrons need more energy to overcome this barrier by an image force (Schottky effect) during the set process. On the other hand, this process also generate donor defects (oxygen vacancies) in the films by repulsing the oxygens to the anode (top electrode) and these defects rearrange themselves to form a conduction path for the electrons and the conduction at the high voltage region is dominated by FPE mechanism. Hereafter, the set process is finished by a current jump and and the LRS curve is dominated by the ohmic conduction whic indicates that stronger filaments are succesfully formed in the devices having the higher Co concentration.

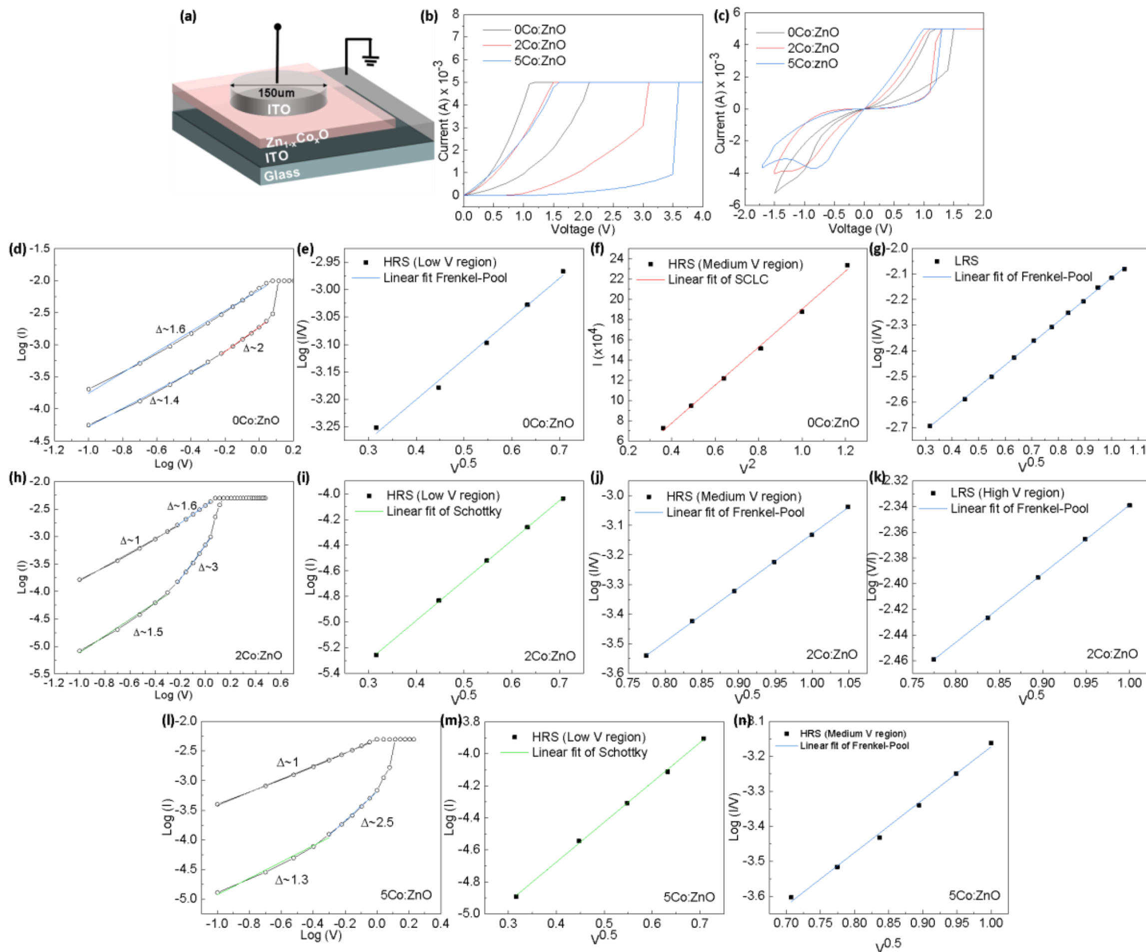

Figure 3. a) Schematic of Co-doped ZnO memristive device structure. Typical I-V curves of Co-doped ZnO memristive devices during: b) forming and c) set-reset processes. d) Log-log curve of set process of 0Co:ZnO device and its conduction mechanism in: e) low and f) medium voltage regions of the HRS curve, and at g) LRS curve. h) log-log curve of set process of 2Co:ZnO device and its conduction mechanism in: i) low and j) medium voltage regions of the HRS curve, and k) high voltage region of LRS. l) Log-log curve of set process of 5Co:ZnO device and its conduction mechanism in m) low and n) medium voltage regions of the HRS curve.

4. Conclusion

The devices made with pure ZnO films have high number of donor defects and the electrons can easily flow from cathode to anode by hopping through these defects and thus the set process was dominated by FPE and SCLC mechanism. It is also found that the low resistance state still follows FPE which we can assume the filament formation is relatively weak. Conversely, the introduction of Co dopants in the ZnO lattice system generates the formation of acceptor defects and the set process is started with Schottky emission which indicates that there is a significant barrier at the electrode/dielectric interface. Consequently, the electron requires higher energy to surpass this Schottky barrier height and induce the formation of strong filaments.

5. Acknowledgement

This work was supported in part by the Ministry of Science and Technology, Taiwan, under project MOST 105-2221-E-009-134-MY3 and NCTU visiting research fellowship program. F. M. Simanjuntak

and T. Prodromakis acknowledge the support of EPSRC Programme Grant (EP/R024642/1) and H2020-FETPROACT-2018-01 SYNCH project.

6. References

[1] Simanjuntak F M, Chandrasekaran S, Lin C and Tseng T-Y 2019 ZnO2/ZnO bilayer switching film for making fully transparent analog memristor devices *APL Materials* **7** 051108

[2] Simanjuntak F M, Ohno T, Chandrasekaran S, Tseng T-Y and Samukawa S 2020 Neutral oxygen irradiation enhanced forming-less ZnO-based transparent analog memristor devices for neuromorphic computing applications *Nanotechnology* **31** 26LT01

[3] Chandrasekaran S, Simanjuntak F, Saminathan R, Panda D and Tseng T-Y 2019 Improving linearity by introducing Al in HfO2 as memristor synapse device *Nanotechnology* **6** 107–13

[4] Chandrasekaran S, Simanjuntak F M, Panda D and Tseng T-Y 2019 Enhanced Synaptic Linearity in ZnO-Based Invisible Memristive Synapse by Introducing Double Pulsing Scheme *IEEE Transactions on Electron Devices* **66** 4722–6

[5] Simanjuntak F M, Chandrasekaran S, Gapsari F and Tseng T Y 2019 Switching and synaptic characteristics of AZO/ZnO/ITO valence change memory device *IOP Conference Series: Materials Science and Engineering* **494** 012027

[6] Simanjuntak F M, Chandrasekaran S, Pattanayak B, Lin C-C and Tseng T-Y 2017 Peroxide induced volatile and non-volatile switching behavior in ZnO-based electrochemical metallization memory cell *Nanotechnology* **28** 38LT02

[7] Chandrasekaran S, Simanjuntak F M, Aluguri R and Tseng T 2018 The impact of TiW barrier layer thickness dependent transition from electro-chemical metallization memory to valence change memory in ZrO2-based resistive switching random access memory devices *Thin Solid Films* **660** 777–81

[8] Simanjuntak F M, Chandrasekaran S, Lin C-C and Tseng T-Y 2018 Switching Failure Mechanism in Zinc Peroxide-Based Programmable Metallization Cell *Nanoscale Research Letters* **13** 327

[9] Singh P, Simanjuntak F M, Kumar A and Tseng T 2018 Resistive switching behavior of Ga doped ZnO-nanorods film conductive bridge random access memory *Thin Solid Films* **660** 828–33

[10] Rajasekaran S, Simanjuntak F M, Panda D, Chandrasekaran S, Aluguri R, Saleem A and Tseng T-Y 2020 Fast, Highly Flexible, and Transparent TaO x -Based Environmentally Robust Memristors for Wearable and Aerospace Applications *ACS Applied Electronic Materials* acsaelm.0c00441

[11] Chandrasekaran S, Simanjuntak F M and Tseng T 2018 Controlled resistive switching characteristics of ZrO 2 -based electrochemical metallization memory devices by modifying the thickness of the metal barrier layer *Japanese Journal of Applied Physics* **57** 04FE10

[12] Simanjuntak F M, Singh P, Chandrasekaran S, Lumbantoruan F J, Yang C-C, Huang C-J, Lin C-C and Tseng T-Y 2017 Role of nanorods insertion layer in ZnO-based electrochemical metallization memory cell *Semiconductor Science and Technology* **32** 124003

[13] Aluguri R, Kumar D, Simanjuntak F M and Tseng T-Y 2017 One bipolar transistor selector - One resistive random access memory device for cross bar memory array *AIP Advances* **7** 095118

[14] Chandrasekaran S, Simanjuntak F M, Tsai T-L, Lin C-A and Tseng T-Y 2017 Effect of barrier layer on switching polarity of ZrO2-based conducting-bridge random access memory *Applied Physics Letters* **111** 113108

[15] Panda D, Simanjuntak F M and Tseng T-Y 2016 Temperature induced complementary switching in titanium oxide resistive random access memory *AIP Advances* **6** 075314

[16] Simanjuntak F M, Ohno T and Samukawa S 2019 Neutral Oxygen Beam Treated ZnO-Based Resistive Switching Memory Device *ACS Applied Electronic Materials* **1** 18–24
[17] Simanjuntak F M, Ohno T and Samukawa S 2019 Influence of rf sputter power on ZnO film characteristics for transparent memristor devices *AIP Advances* **9** 105216
[18] Simanjuntak F M, Pattanayak B, Lin C-C and Tseng T-Y 2017 Resistive Switching Characteristics of Hydrogen Peroxide Surface Oxidized ZnO-Based Transparent Resistive Memory Devices *ECS Transactions* **77** 155–60
[19] Simanjuntak F M, Panda D, Wei K and Tseng T 2016 Status and Prospects of ZnO-Based Resistive Switching Memory Devices *Nanoscale Research Letters* **11** 368
[20] Simanjuntak F M, Panda D, Tsai T-L, Lin C-A, Wei K-H and Tseng T-Y 2015 Enhancing the memory window of AZO/ZnO/ITO transparent resistive switching devices by modulating the oxygen vacancy concentration of the top electrode *Journal of Materials Science* **50** 6961–9
[21] Simanjuntak F M, Panda D, Tsai T-L, Lin C-A, Wei K-H and Tseng T-Y 2015 Enhanced switching uniformity in AZO/ZnO 1−x /ITO transparent resistive memory devices by bipolar double forming *Applied Physics Letters* **107** 033505
[22] Simanjuntak F M, Ohno T and Samukawa S 2019 Film-Nanostructure-Controlled Inerasable-to-Erasable Switching Transition in ZnO-Based Transparent Memristor Devices: Sputtering-Pressure Dependency *ACS Applied Electronic Materials* **1** 2184–9
[23] Panda D, Simanjuntak F M, Chandrasekaran S, Pattanayak B, Singh P and Tseng T Y 2020 Barrier Layer Induced Switching Stability in Ga:ZnO Nanorods Based Electrochemical Metallization Memory *IEEE Transactions on Nanotechnology* 1–1
[24] Simanjuntak F M, Prasad O K, Panda D, Lin C-A, Tsai T-L, Wei K-H and Tseng T-Y 2016 Impacts of Co doping on ZnO transparent switching memory device characteristics *Applied Physics Letters* **108** 183506
[25] Chiu F 2014 A Review on Conduction Mechanisms in Dielectric Films *Advances in Materials Science and Engineering* **2014** 1–18
[26] Lim E and Ismail R 2015 Conduction Mechanism of Valence Change Resistive Switching Memory: A Survey *Electronics* **4** 586–613